

# MnO Spin-Wave Dispersion Curves from Neutron Powder Diffraction Data

Andrew L. Goodwin,<sup>1</sup> Martin T. Dove,<sup>1</sup> Matthew G. Tucker,<sup>2</sup> and David A. Keen<sup>2,3</sup>

<sup>1</sup>*Department of Earth Sciences, Cambridge University, Downing Street, Cambridge CB2 3EQ, U.K.*

<sup>2</sup>*ISIS Facility, Rutherford Appleton Laboratory, Chilton, Didcot, Oxfordshire OX11 0QX, U.K.*

<sup>3</sup>*Department of Physics, Oxford University, Clarendon Laboratory, Parks Road, Oxford OX1 3PU, U.K.*

(Dated: June 28, 2018)

We describe a model-independent approach for the extraction of spin-wave dispersion curves from neutron total scattering data. The method utilises a statistical analysis of real-space spin configurations to calculate spin-dynamical quantities. The RMCProfile implementation of the reverse Monte Carlo refinement process is used to generate a large ensemble of supercell spin configurations from powder diffraction data. Our analysis of these configurations gives spin-wave dispersion curves that agree well with those determined independently using neutron triple-axis spectroscopic techniques.

PACS numbers: 75.30.Ds, 61.12.Bt, 02.70.Uu

In this Letter, we explore the unexpected possibility that neutron powder diffraction might be used to probe spin *dynamics* in magnetic materials. In effect, what we are asking is whether there is sufficient information preserved in experimentally observed neutron scattering functions to allow reconstruction of the spin-wave dispersion.

It is well known that the intensities of magnetic Bragg reflections are determined entirely by one-particle correlations (the same is true, naturally, for the nuclear Bragg reflections). In terms of spin-dynamical information, these describe the average fluctuations in moment at each magnetic site. However, any determination of spin-wave dispersion relations would require access to the two-particle spin correlation functions. For this reason, we have focussed our efforts on an analysis of the *total* magnetic neutron scattering patterns, considering both elastic (which includes Bragg) and inelastic (included in the diffuse) components alike [4, 5]. This is because the latter cannot be described effectively without recourse to the two-particle correlation functions; indeed, all the spin-dynamical information is folded into the total scattering process. What is not clear is the extent to which the orientational averaging implicit in powder diffraction experiments complicates—or indeed precludes—recovery of this information. Our paper aims to address the two issues so raised: (i) to what extent are the two-particle spin correlations preserved in total neutron scattering data, and (ii) how might one extract these correlations in practice, and in doing so determine spin-wave dispersion relations? The potential impact of a robust methodology based on neutron powder diffraction is significant, particularly since spin-wave information could be rapidly obtained from *e.g.* newly-discovered polycrystalline materials and/or those materials for which a route to large single crystal samples does not exist.

A similar problem—one that has received more widespread attention—is that of extracting phonon dispersion curves from the neutron powder diffraction patterns of non-magnetic materials [1, 2, 3]. On the one

hand, the extraction of spin-waves might be expected to prove more tractable, in that the number of spin-wave modes in a material is always less than the number of phonon modes, and the absolute energies of spin-waves tend to be lower than most phonon energies (and hence their signature within diffraction data should be clearer). On the other hand, the analysis of diffraction data from magnetic materials will be complicated both by the superposition of nuclear and magnetic scattering contributions and by the magnetic form-factor dependence. What is clear—and this has emerged in the development of methods for extracting phonons from diffraction—is the need for model-independent approaches, so that the answers one obtains are driven by data rather than the choice of any particular dynamical model [2, 3].

This paper describes a “proof of principle” investigation into the possibility of extracting spin-wave dispersion curves from powder diffraction data. We present results for manganese(II) oxide (MnO) that indicate one can indeed recover the spin-wave excitation spectrum for this system, albeit with some identifiable yet surmountable limitations. Our paper begins by describing the reverse Monte Carlo (RMC) method of refining total neutron scattering data. We proceed to illustrate how statistical analysis of large ensembles of these RMC configurations can yield quantitative measurements of the spin-wave dispersion. Our diffraction-based MnO spin-wave dispersion curves are presented and compared with those obtained independently using triple-axis inelastic neutron spectroscopy. We close with a discussion of some necessary developments for the approach to offer a viable method of measuring spin-wave dispersion curves in materials for which established techniques are impractical.

For non-magnetic materials, the Fourier transform of the observed total scattering data gives the real-space atomic pair distribution function, which contains detailed information regarding the local structural environments present in the sample. The RMC method provides a particularly effective means of analysing total scattering data, in that it can be used to refine atomistic configura-

tions that represent large supercells of the known structural unit cell [6, 7]. These supercells reflect simultaneously the average periodic structure (as given by the observed Bragg intensities) together with the collective displacements from which the diffuse scattering arises. We have shown elsewhere that these atomic displacements are well described as an instantaneous superposition of all phonon modes [2, 3].

Magnetic materials require refinement of both atomistic and spin configurations to account for the observed scattering function. We have recently extended the RMCProfile implementation of the RMC method to allow simultaneous modelling of nuclear and magnetic structures [8]. The procedure, which is described in detail elsewhere [4, 8], involves minimisation of the “mismatch” function

$$\chi_{\text{RMC}}^2 = \chi_{S(Q)}^2 + \chi_{\text{Bragg}}^2, \quad (1)$$

where

$$\begin{aligned} \chi_{S(Q)}^2 &= \sum_k \sum_j [S_{\text{calc}}(Q_j)_k - S_{\text{exp}}(Q_j)_k]^2 / \sigma_k^2(Q_j), \\ \chi_{\text{Bragg}}^2 &= \sum_i [I_{\text{calc}}(t_i) - I_{\text{exp}}(t_i)]^2 / \sigma^2(t_i). \end{aligned} \quad (2)$$

Here,  $S(Q)$  is the observed scattering function as measured in each of  $k$  data sets (such as from a range of detector banks, for example), and  $I(t)$  is the time-of-flight Bragg powder profile as described in more detail elsewhere [7]. The function  $\chi_{\text{RMC}}^2$  is minimised by successive random moves of two sorts: displacement of atoms in the atomistic configuration and re-orientation of individual spin vectors in the associated spin configuration. Such moves are continually generated and accepted or rejected according to the Monte Carlo algorithm until the fit-to-data does not improve further. At this point, one has a pair of configurations (one atomistic, one spin) that reflects both nuclear and magnetic contributions to the Bragg *and* diffuse scattering patterns. As such, we can expect the RMC spin orientations to represent an instantaneous superposition of the spin-wave modes: a “snapshot” of the spin dynamics. The essence of our analysis is to collect large numbers of these spin configurations, so as to sample many different “snapshots” of the spin-dynamical motion. By probing the various spin correlations that recur, and the frequency with which they do so, we will show how one can reconstruct spin-wave dispersion curves from such ensembles.

We have elected to use MnO as a case-study in this investigation as its magnetic structure and spin dynamics have been the focus of a large body of systematic investigation [8, 9, 10, 11, 12]. It is widely considered a benchmark antiferromagnetic material, and is commonly used as a representative of the family of first-row transitional-metal oxides in a variety of theoretical studies. A paramagnet at room temperature, MnO exhibits

long-range antiferromagnetic ordering at temperatures below  $T_N = 118$  K. Its paramagnetic to antiferromagnetic transition is accompanied by a distortion of the high-temperature cubic lattice to a monoclinic variant with pseudo-rhombohedral geometry. The basic antiferromagnetic structure of MnO can be described in terms of a single spin-alignment axis, and its spin dynamics are well-understood in terms of simple Heisenberg interactions.

We collected neutron total scattering data for a powdered sample of MnO using the GEM instrument at ISIS [13]. The experiment spanned a range of momentum transfers  $0.3 < Q < 50 \text{ \AA}^{-1}$  and was performed at a temperature of 100 K. We expected the increased relative magnitude of spin displacements at this temperature to facilitate our analysis: a study at more “conventional” temperatures (*e.g.*, where the spin excitation energies are less broad) would place a greater emphasis on resolution effects than proof of concept. Raw data were converted to  $S(Q)$  and Bragg intensity data for use as input for the RMC procedure. We used the RMCProfile program to refine an ensemble of *ca* 600 RMC configurations, each of which contained a  $20 \times 20 \times 20$  array of fcc unit cells (*i.e.*, a  $10 \times 10 \times 10$  array of conventional magnetic unit cells, containing 32 000 Mn atoms). Our starting configurations were prepared by assigning to each atom a small random displacement from its average position; the spin orientations were also varied in a similar fashion. For consistency with previous spin-wave investigations [10, 11, 12], we neglected any deviations from cubic lattice symmetry; this simplification is known to have little effect on the associated analysis. Each pair of equilibrium configurations were separated by a minimum of 150 000 RMC “moves” [14], so that they might be considered essentially independent for our analysis.

A method of extracting spin-dynamical information from ensembles of spin configurations will be published in detail elsewhere [15]; there is a strong analogy to the known methods of extracting lattice-dynamical information from atomistic configurations [16]. Here we describe the most pertinent aspects of the theory. The analysis begins by calculating for each configuration (labelled  $t$ ) a number of collective variables of the form

$$\tau(j, \mathbf{k}, t) = \sqrt{\frac{\hbar S_j}{2N}} \sum_{\ell} \sigma^+(j\ell, t) \exp[i\mathbf{k} \cdot \mathbf{r}(j\ell)]. \quad (3)$$

There will be one of these variables for each of the  $Z$  spins in the (primitive) magnetic unit cell. Here,  $S_j$  is the spin quantum number of the spin type  $j$ ,  $\mathbf{r}(j\ell)$  its average position in unit cell  $\ell$ , and  $\sigma^+(j\ell, t)$  a parameter that describes the deviation from the average spin alignment axis. All  $Z$  collective variables at each wave-vector  $\mathbf{k}$  are assembled into the one column vector  $\boldsymbol{\tau}(\mathbf{k}, t)$ . This quantity is related to the Holstein-Primakoff magnon variable

$\mathbf{b}_{\mathbf{k}}(t)$  [17] via the mapping

$$\sqrt{\hbar}\mathbf{b}_{\mathbf{k}}(t) = \mathbf{A}(\mathbf{k}) \cdot \boldsymbol{\tau}(\mathbf{k}, t). \quad (4)$$

Here, the change of basis occurs between the normal mode coordinates (the basis of  $\mathbf{b}$ ) and the spin-type coordinates (the basis of  $\boldsymbol{\tau}$ ), and is given by the ( $t$ -independent) matrix  $\mathbf{A}$ , itself constructed from the spin-wave mode displacement vectors [15].

We proceed by calculating the  $t$ -averaged matrix  $\boldsymbol{\Sigma}$ ,

$$\boldsymbol{\Sigma}(\mathbf{k}) = \langle \boldsymbol{\tau}^*(\mathbf{k})\boldsymbol{\tau}^T(\mathbf{k}) \rangle. \quad (5)$$

This representation is useful because it allows us to exploit the orthonormality of the basis for  $\mathbf{b}$ : in particular, the matrix  $\mathbf{b}_{\mathbf{k}}^*(t)\mathbf{b}_{\mathbf{k}}^T(t)$  is diagonal with entries given by the mode occupation numbers  $n(\mathbf{k})$  [17]. Substitution of Eq. (4) into Eq. (5) gives

$$\mathbf{A}(\mathbf{k}) \cdot \boldsymbol{\Sigma}(\mathbf{k}) \cdot \mathbf{A}^T(\mathbf{k}) = \hbar \langle \mathbf{b}_{\mathbf{k}}^* \mathbf{b}_{\mathbf{k}}^T \rangle. \quad (6)$$

Since  $\hbar \langle \mathbf{b}_{\mathbf{k}}^* \mathbf{b}_{\mathbf{k}}^T \rangle$  is diagonal, its elements [the  $\hbar n(\mathbf{k})$ ] are given by the eigenvalues  $e_i(\mathbf{k})$  of  $\boldsymbol{\Sigma}(\mathbf{k})$ . In this way, diagonalisation of  $\boldsymbol{\Sigma}$ , a matrix that can be constructed (via the  $\boldsymbol{\tau}$ ) entirely from observed spin displacements in RMC configurations, yields the spin-wave occupation numbers. The spin-wave frequencies may then be calculated in a straightforward manner:

$$\omega_i(\mathbf{k}) = \frac{k_B T}{\hbar} \ln \left[ \frac{\hbar}{e_i(\mathbf{k})} + 1 \right]. \quad (7)$$

By repeating this analysis for a range of wave-vectors, one may construct a set of spin-wave dispersion curves from the RMC configurations. The number of  $\mathbf{k}$ -points included in these dispersion curves is limited by the configurational box size used (which in turn is limited by the available computational resources): a box representing  $n_a, n_b, n_c$  unit cells along axes  $\mathbf{a}, \mathbf{b}, \mathbf{c}$  permits the set of wave-vectors

$$\mathbf{k} = \frac{i_a}{n_a} \mathbf{a}^* + \frac{i_b}{n_b} \mathbf{b}^* + \frac{i_c}{n_c} \mathbf{c}^* \quad i_a, i_b, i_c \in \mathbb{Z}. \quad (8)$$

We proceeded to apply this analysis to our ensemble of MnO configurations, calculating spin-wave frequencies across the  $[\bar{\xi}\bar{\xi}\xi]$ ,  $[\xi\xi\xi]$ ,  $[00\xi]$  and  $[\xi\xi 0]$  directions of reciprocal space—these being the axes for which inelastic neutron scattering (INS) data were available for comparison [10, 11]. The  $\mathbf{k}$ -point mesh size (0.1 r.l.u.) was limited by the number of magnetic—rather than nuclear—unit cells in the configuration. Calculation at symmetry-equivalent wave-vectors enabled determination of the errors involved. While we observed two distinct spin-wave modes at each wave-vector, inspection of the associated mode displacement vectors revealed that their relative order in the spin-wave spectrum was not consistent. This is unsurprising given that the energies of the

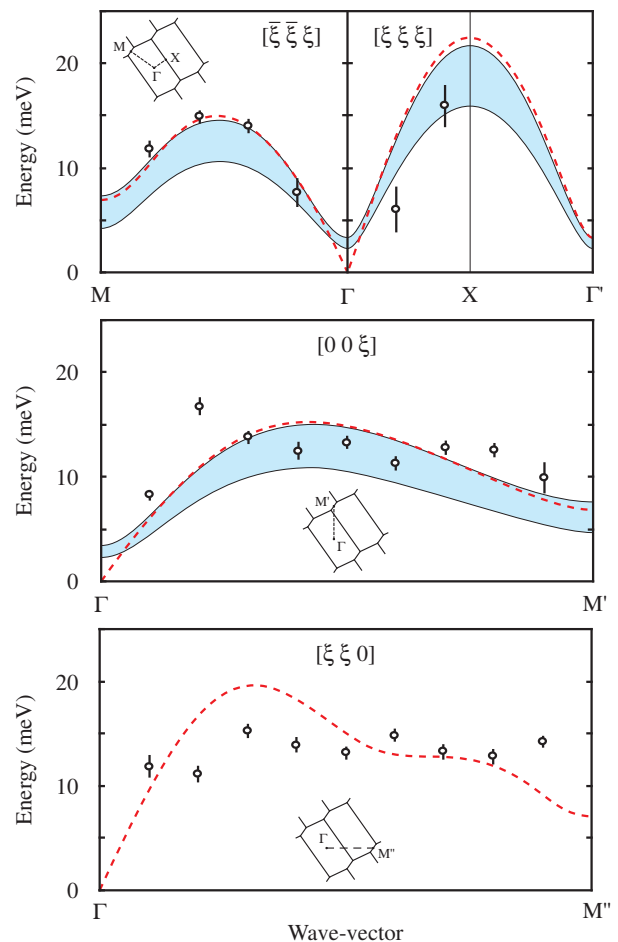


FIG. 1: (Colour online) MnO spin-wave dispersion curves calculated from our RMC configurations (data points). Fits to the INS data of Pepy [10] (shaded regions,  $88.75 \text{ K} \leq T \leq 113.75 \text{ K}$ ) and of Kohgi [11] (red dashed lines,  $T = 100 \text{ K}$ ) are included for comparison. The relevant directions in reciprocal space are illustrated on a  $(1\bar{1}0)$  section of the MnO reciprocal lattice.

two modes are known to be essentially identical at most wave-vectors [10, 11, 12]. Consequently, the frequencies obtained were also averaged over both branches. Our results [Fig. 1] are compared here to the dispersion curves given in previous INS studies. Pepy gives data for the  $[\bar{\xi}\bar{\xi}\xi]$ ,  $[\xi\xi\xi]$  and  $[00\xi]$  branches at 88.75 K and 113.75 K, which serve as upper and lower bounds respectively to the expected energy spectrum [10]; Kohgi *et al.* report data at 100 K, from which they were able to calculate dispersion curves along the same three branches together with the  $[\xi\xi 0]$  direction [11]. Collins *et al.* give data at only at 4.2 K [12]; as there is some significant temperature dependence in the dispersion, these results are not considered further. The curves shown in Fig. 1 are taken from the spin-interaction models described in the original reports, refined by fitting to the observed INS data. The magnon peaks can be relatively broad at such tempera-

tures, making absolute energies difficult to assign [10, 11]. Indeed it is interesting that the models differ somewhat in their overall energy scale and in the behaviour of the spin-wave energies near the zone centre.

Our purpose in comparing our calculations with the results of INS experiments is to establish whether it is at all possible to extract a similar level of spin-dynamical information from diffraction data. In this sense, it is promising that the spin-wave energies we calculate from our RMC configurations agree well with the overall energy scale observed in INS studies: the level of correlated spin “motion” in our RMC configurations is appropriate for the given temperature and actual spin-wave energies. Moreover, there is some clear evidence for variation in spin-wave frequency with wave-vector. Certainly, the form of the  $[\bar{\xi}\bar{\xi}\xi]$  and  $[\xi\xi\xi]$  branches—and to a lesser extent that of the  $[00\xi]$  branch—follows closely that of the INS-based models. In addition to the general form of the dispersion curves, one very encouraging feature is the apparent increase in spin-wave energy at the M-point relative to the zone centre, which reflects the known inequivalence of parallel and anti-parallel nearest-neighbour couplings. However, there are regions where the similarity between our dispersion curves and those determined using INS is less precise: our data along  $[\xi\xi0]$  show relatively little dispersion, but do occur over an appropriate energy range. It is not immediately obvious why the diffraction data should be more sensitive to some regions of the magnon dispersion than others; what is known is that modes at different wave-vectors can contribute to differing extents to the real-space distribution functions [3].

Despite our employment of state-of-the-art computational resources, the RMC configurations prepared were not sufficiently large to determine the precise dispersion behaviour near the BZ origin. The existence of “gaps”, their anisotropy and temperature dependence are often important features of spin-wave spectra, and a method would have to reflect these to be of general use. However a limitation of  $\mathbf{k}$ -point mesh size is one that can be expected to abate as computational power increases. Other, more inherent, limitations will exist. For example, it is likely that there is some maximum observable spin-wave energy: this is certainly true for phonon frequencies [3], and magnons suffer additionally from the restricted  $Q$ -range over which magnetic scattering is observable.

At this “proof of principle” stage, the important result is that it is possible to retrieve even broad features of the spin-wave dispersion from powder diffraction data. Already, one might argue that relatively sensible parameters for a spin interaction model could be extracted from dispersion curves such as those in Fig. 1, given that some features of the dispersion are well described, and those that are less-well fixed by the data might often be constrained by our understanding of spin dynamics. Moreover, the accuracy of the magnon dispersion curves deter-

mined from diffraction data can be expected to improve significantly. Our methods of treating the very high quality data one obtains from instruments such as GEM will improve; access to sufficient computational power will increase. The potential for powder diffraction experiments to allow determination of spin-wave excitation spectra is itself an important result: it provides a possible mechanism for the exploration of spin dynamics in newly-characterised materials, for which single crystal samples are not immediately available.

We acknowledge financial support from EPSRC (U.K.), and from Trinity College, Cambridge to A.L.G.

- 
- [1] D. A. Dimitrov, D. Louca, H. Röder, Phys. Rev. B **60**, 6204 (1999); W. Reichardt, L. Pintschovius, Phys. Rev. B **63**, 174302 (2001); M. J. Graf, I.-K. Jeong, D. L. Starr, R. H. Heffner, Phys. Rev. B **68**, 064305 (2003); I.-K. Jeong, R. H. Heffner, M. J. Graf, S. J. L. Billinge, Phys. Rev. B **67**, 104301 (2003).
  - [2] A. L. Goodwin, M. G. Tucker, M. T. Dove, D. A. Keen, Phys. Rev. Lett. **93**, 075502 (2004); **95**, 119901(E) (2005)
  - [3] A. L. Goodwin, M. G. Tucker, E. R. Cope, M. T. Dove, D. A. Keen, Phys. Rev. B **72**, 214304 (2005).
  - [4] M. T. Dove, M. G. Tucker, D. A. Keen, Eur. J. Miner. **14**, 331 (2002).
  - [5] V. M. Nield, D. A. Keen, *Diffuse Neutron Scattering from Crystalline Materials* (Oxford University Press, Oxford, England, 2001); T. Egami, S. J. L. Billinge, *Underneath the Bragg Peaks: Structural Analysis of Complex Materials* (Pergamon Press, Oxford, England, 2003).
  - [6] R. L. McGreevy, J. Phys.: Condens. Matter **13**, R887 (2001)
  - [7] D. A. Keen, M. G. Tucker, M. T. Dove, J. Phys.: Condens. Matter **17**, S15 (2005).
  - [8] A. L. Goodwin, M. G. Tucker, M. T. Dove, D. A. Keen, Phys. Rev. Lett. **96**, 047209 (2006).
  - [9] W. L. Roth, Phys. Rev. **110**, 1333 (1958); H. Shaked, J. Faber, Jr., R. L. Hitterman, Phys. Rev. B **38**, 11901 (1988); D. Hohlwein, J.-U. Hoffmann, R. Schneider, Phys. Rev. B **68**, 140408(R) (2003).
  - [10] G. Pepy, J. Phys. Chem. Solids, **35**, 433 (1974).
  - [11] M. Kohgi, Y. Ishikawa, I. Harada, K. Motizuki, J. Phys. Soc. Jpn. **36**, 112 (1974).
  - [12] M. F. Collins, V. K. Tondon, W. J. L. Buyers, Int. J. Magn. **4**, 17 (1973).
  - [13] A. C. Hannon, Nucl. Instrum. Meth. A **551**, 88 (2005).
  - [14] The separation of RMC configurations containing  $N$  atoms by at least  $N \ln 10$  “moves” ensures that the positions or orientations of at least 90% of atoms or spins differ from configuration to configuration.
  - [15] A. L. Goodwin, M. T. Dove, M. G. Tucker, D. A. Keen, arXiv:cond-mat/0601559.
  - [16] M. T. Dove and R. M. Lynden-Bell, Philos. Mag. B **54**, 443 (1986); M. T. Dove, *Introduction to Lattice Dynamics* (Cambridge University Press, Cambridge, England, 1993).
  - [17] T. Holstein and H. Primakoff, Phys. Rev. **58**, 1098 (1940).